Matlab/Simulink Based on $\alpha\beta$ Modeling of Self-Excited Induction Generator

Y. Kumsuwan[1] W. Srirattanawichaikul[2] and S. Premrudeepreechacharn[2]
[1]Department of Electrical Engineering, Rajamangala University of Technology Lanna Tak Campus, Tak, Thailand
Email: yuttana@doe1.eng.cmu.ac.th
[2]Department of Electrical Engineering, Faculty of Engineering, Chiang Mai University, Chiang Mai, Thailand
Email: g500631047@doe1.eng.cmu.ac.th, sutticha@doe1.eng.cmu.ac.th

Abstract

This paper presents modeling of stand-alone self-excited induction generator used to operate under variable speeds prime mover. The proposed dynamic model consists of induction generator, excitation capacitor and inductive load model are expressed in stationary α–β reference frame with the actual magnetizing saturation curve of the induction machine. The aim of this research is to developed and designs of the self-excited induction generator and to describe the simulation results using a Matlab/Simulink. The system has been simulated to verify its capability such as build-up voltage and stator flux linkage responses, stator phase current, electromagnetic torque and variation of magnetizing inductance both during dynamic and steady-state with variable speed prime mover.

Keywords: self-excited induction generator, dynamic model, Matlab/Simulink.

1. Introduction

Nowadays, self-excited induction generator (SEIG), shown in Fig. 1, using induction machines is widely recognized [1]-[3]. The SEIG has many advantages over the DC generator and the synchronous generator for example: robust and brushless (squirrel-cage rotor) construction, ruggedness, ease of maintenance, absence of DC power supply for field excitation, reduced unit cost and size, better transient performance, self-protection against short-circuits and large over loads, etc. However, the major drawbacks of SEIG are reactive power consumption, its relatively poor voltage and frequency regulation under varying prime mover speed, excitation capacitor and load characteristics [1].

In [3] the dynamic characteristic of an isolated SEIG driven by a wind turbine is studied, the SIMNON simulation software presented the effect of magnetizing inductance on self-excitation. In [4] novel voltage controllers for stand-alone induction generator, in which PWM-VSI are used. In [5] a method is proposed for accurately predicting the minimum value of capacitance necessary to initiate self-excitation with a stand-alone induction generator. It offers good steady-state and transient performance with build-up of generate voltage, and the perturbations of the terminal voltage and the stator current which result from load change. However, this technique has limitation in being computationally intensive.

This paper presents the design and simulation of SEIG with Matlab/Simulink. The proposed method is applicable to both steady-state and transient of SEIG with variable speed prime mover. This method is based on the analysis of the dynamic α–β reference frame model of the SEIG with a general inductive load connected to its terminal. The mathematical modeling of SEIG, presented in Section 2, is based on stationary reference frame. A simulation model consisting of the induction generator, the excitation capacitor, and load is presented in Section 3. To evaluate the performance of the proposed approach, computer simulation is presented in Section 4. Finally, Section 5 concludes this paper.

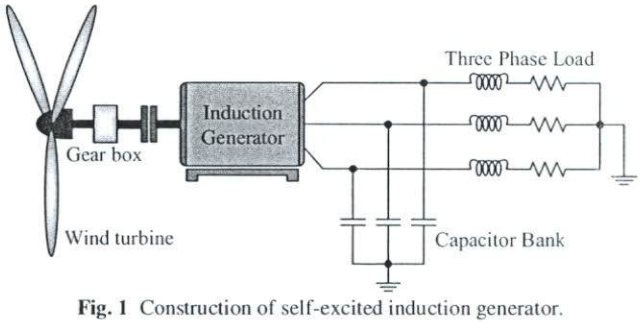

Fig. 1 Construction of self-excited induction generator.

2. Modeling of Self-Excited Induction Generator

From Fig. 1, the induction machine can operate as a SEIG if a suitable capacitor bank is connected across its stator terminals and its rotor is driven at a suitable speed by an external prime mover such as wind energy, biogas, mini/micro-hydro, etc. In addition, the process of build-up voltage in an induction generator is very much similar to that of a DC generator. There must be a suitable value of residual magnetism presented in the rotor [6],[7]. Fig. 2 shows the α–β equivalent circuit of the SEIG in the stationary reference frame.

2.1 Dynamic Model

The dynamic model of SEIG in stationary reference frame can be written in α–β reference frame variables. Components stator and rotor voltage of the induction motor can be expressed as follows [8]:

$$v_{s\alpha} = R_s i_{s\alpha} + L_s \frac{d}{dt} i_{s\alpha} + L_m \frac{d}{dt} i_{r\alpha} \quad (1)$$

$$v_{s\beta} = R_s i_{s\beta} + L_s \frac{d}{dt} i_{s\beta} + L_m \frac{d}{dt} i_{r\beta}, \quad (2)$$

$$0 = R_r i_{r\alpha} + L_r \frac{di_{r\alpha}}{dt} + L_m \frac{di_{s\alpha}}{dt} + \omega_r \psi_{r\beta} \quad (3)$$

$$0 = R_r i_{r\beta} + L_r \frac{d}{dt} i_{r\beta} + L_m \frac{d}{dt} i_{s\beta} - \omega_r \psi_{r\alpha}. \quad (4)$$

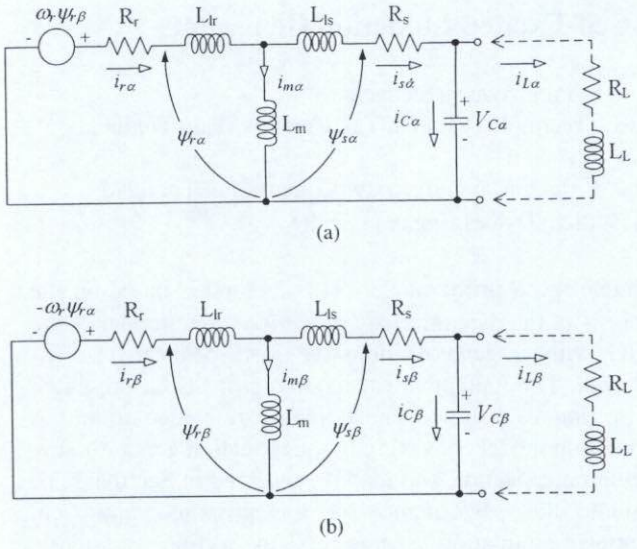

Fig. 2 Equivalent circuit of SEIG (a) α-axis (b) β-axis

The expressions for capacitor voltages are

$$V_{C\alpha} = \frac{1}{C}\int i_{C\alpha}dt + V_{C\alpha 0}, \tag{5}$$

$$V_{C\beta} = \frac{1}{C}\int i_{C\beta}dt + V_{C\beta 0}. \tag{6}$$

The components of rotor flux linkage in the stationary reference can be written as

$$\psi_{r\alpha} = L_m i_{s\alpha} + L_r i_{r\alpha} + \psi_{r\alpha 0}, \tag{7}$$

$$\psi_{r\beta} = L_m i_{s\beta} + L_r i_{r\beta} + \psi_{r\beta 0}. \tag{8}$$

where $\psi_{r\alpha 0}$ and $\psi_{r\beta 0}$ are the residual rotor flux linkages in α–β axis, respectively.

Then, with an electrical rotor speed of ω_r, the components of rotating voltage in the stationary reference frame are as follows:

$$\omega_r\psi_{r\alpha} = \omega_r L_m i_{s\alpha} + \omega_r L_r i_{r\alpha} + \omega_r\psi_{r\alpha 0}, \tag{9}$$

$$\omega_r\psi_{r\beta} = \omega_r L_m i_{s\beta} + \omega_r L_r i_{r\beta} + \omega_r\psi_{r\beta 0}. \tag{10}$$

Using Fig. 2 and equations (1)-(10), for the matrix equations of SEIG at no-load in the stationary reference frame are given by

$$\begin{bmatrix}0\\0\\0\\0\end{bmatrix} = \begin{bmatrix} R_s + pL_s & 0 & pL_m & 0 \\ 0 & R_s + pL_s & 0 & pL_m \\ pL_m & \omega_r L_m & R_r + pL_r & \omega_r L_r \\ -\omega_r L_m & pL_m & -\omega_r L_r & R_r + pL_r \end{bmatrix} \begin{bmatrix} i_{s\alpha} \\ i_{s\beta} \\ i_{r\alpha} \\ i_{r\beta} \end{bmatrix} + \begin{bmatrix} V_{C\alpha} \\ V_{C\beta} \\ \omega_r\psi_{r\beta 0} \\ -\omega_r\psi_{r\alpha 0} \end{bmatrix}. \tag{11}$$

From (11), can be written the state equations as follows:

$$\dot{A}pI_G + BI_G + V_G = 0 \tag{12}$$

where

$$A = \begin{bmatrix} L_s & 0 & L_m & 0 \\ 0 & L_s & 0 & L_m \\ L_m & 0 & L_r & 0 \\ 0 & L_m & 0 & L_r \end{bmatrix}, B = \begin{bmatrix} R_s & 0 & 0 & 0 \\ 0 & R_s & 0 & 0 \\ 0 & \omega_r L_m & R_r & \omega_r L_r \\ -\omega_r L_m & 0 & -\omega_r L_r & R_r \end{bmatrix}, I_G = \begin{bmatrix} i_{s\alpha} \\ i_{s\beta} \\ i_{r\alpha} \\ i_{r\beta} \end{bmatrix}, V_G = \begin{bmatrix} V_{C\alpha} \\ V_{C\beta} \\ \omega_r\psi_{r\beta 0} \\ -\omega_r\psi_{r\alpha 0} \end{bmatrix}.$$

Using matrix inversion, from (12) can be written as

$$pI_G = -A^{-1}BI_G - A^{-1}V_G. \tag{13}$$

From the above equation, the first order differential equations in term the stator and rotor currents can be derived as

$$pi_{s\alpha} = -\frac{L_r}{L}(R_s i_{s\alpha} + V_{C\alpha}) + \frac{L_m}{L}\left[\omega_r(L_m i_{s\beta} + L_r i_{r\beta} + \psi_{r\beta 0}) + R_r i_{r\alpha}\right], \tag{14}$$

$$pi_{s\beta} = -\frac{L_r}{L}(R_s i_{s\beta} + V_{C\beta}) - \frac{L_m}{L}\left[\omega_r(L_m i_{s\alpha} + L_r i_{r\alpha} + \psi_{r\alpha 0}) - R_r i_{r\beta}\right], \tag{15}$$

$$pi_{r\alpha} = \frac{L_m}{L}(R_s i_{s\alpha} + V_{C\alpha}) - \frac{L_s}{L}\left[\omega_r(L_m i_{s\beta} + L_r i_{r\beta} + \psi_{r\beta 0}) + R_r i_{r\alpha}\right], \tag{16}$$

$$pi_{r\beta} = \frac{L_m}{L}(R_s i_{s\beta} + V_{C\beta}) + \frac{L_s}{L}\left[\omega_r(L_m i_{s\alpha} + L_r i_{r\alpha} + \psi_{r\alpha 0}) - R_r i_{r\beta}\right]. \tag{17}$$

where $L = L_s L_r - L_m^{\,2}$.

The differential equations given in (14)-(17) are also used for the applied load condition of the SEIG. For an inductive load (RL) the additional equations needed are:

The components of differential load voltages equation can be written as

$$pv_{L\alpha} = \frac{1}{C}i_{C\alpha}, \tag{18}$$

$$pv_{L\beta} = \frac{1}{C}i_{C\beta}. \tag{19}$$

where $i_{C\alpha} = i_{s\alpha} - i_{L\alpha}$, $i_{C\beta} = i_{s\beta} - i_{L\beta}$.

The components of differential load current equation can be written as

$$pi_{L\alpha} = \frac{1}{L_L}(v_{L\alpha} - R_L i_{L\alpha}), \tag{20}$$

$$pi_{L\beta} = \frac{1}{L_L}(v_{L\beta} - R_L i_{L\beta}). \tag{21}$$

2.2 Magnetizing Inductance and Capacitor on Self-Excitation

As the stator of the SEIG is connected to an isolated load, the magnetizing inductance and stator magnetizing current cannot be considered constant. Because, the variation of magnetizing inductance is the main factor in generate of voltage build-up and stabilization.

The relationship between the magnetizing inductance and magnetizing current is obtained experimentally from open-circuit test at synchronous speed with induction motor parameters listed in Table 1. The magnetizing inductance curves as function of magnetizing current is given in Fig. 3 and it is a nonlinear function of magnetizing current, which can be represented by fifth order polynomial curve fit as in [9].

$$L_m = \frac{1}{120\pi}\begin{bmatrix} -0.1175I_m^{\,5} + 1.918I_m^{\,4} - 11.074I_m^{\,3} + 25.387I_m^{\,2} \\ -19.662I_m + 53.365 \end{bmatrix}, \quad 0 < I_m \le 6.0\text{A} \tag{22}$$

when, the measured magnetizing current is

$$I_m = \sqrt{(i_{s\alpha} + i_{r\alpha})^2 + (i_{s\beta} + i_{r\beta})^2}. \tag{23}$$

From (14) to (17) and (22), the developed electromagnetic torque of SEIG is computed from these current components and magnetizing inductance can be written as

$$T_e = \frac{3}{2} p_p L_m (i_{s\beta} i_{r\alpha} - i_{s\alpha} i_{r\beta}). \tag{24}$$

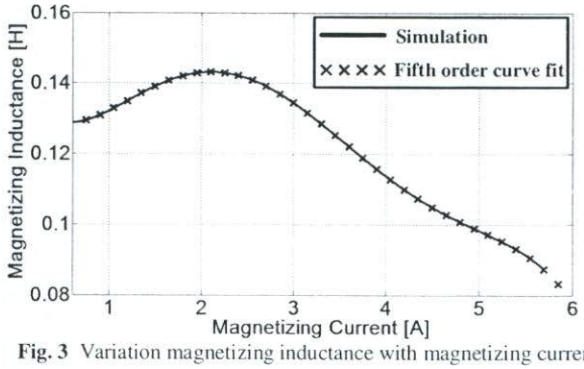

Fig. 3 Variation magnetizing inductance with magnetizing current.

From Fig. 3, the design of capacitor bank of the SEIG, needed to generate the rated voltage under the no-load and the rated speed conditions, the capacitance of the capacitor bank is defined as follows:

$$C_{\min} = \frac{1}{\omega_r^{\,2} L_m}. \tag{25}$$

By substituting (22) into (25), the minimum capacitance for build-up voltage at the rated speed under the no-load is $C_{\min} \cong 50\mu$F, when the unsaturated magnetizing inductance is $L_m = L_{unsaturation} = 141.56$ mH at the rated speed $N_r = 1800$ rpm.

3. Modeling Using Matlab/Simulink

Matlab/Simulink models were developed to examine the SEIG. The equations from (14) to (24) have been implemented in Simulink using different blocks. In this paper the step by step modeling of SEIG has been described.

In Fig. 4, shows the sub-system block of stator and rotor α–β currents. The load voltages and currents block in which stator voltage determined has been shown in Figs. 5 and 6, respectively. Fig. 7 shows the magnetizing current and magnetizing inductance. Fig. 8, shows the electromagnetic torque generated. Finally, In Fig. 9, the Simulink model of SEIG has been shown.

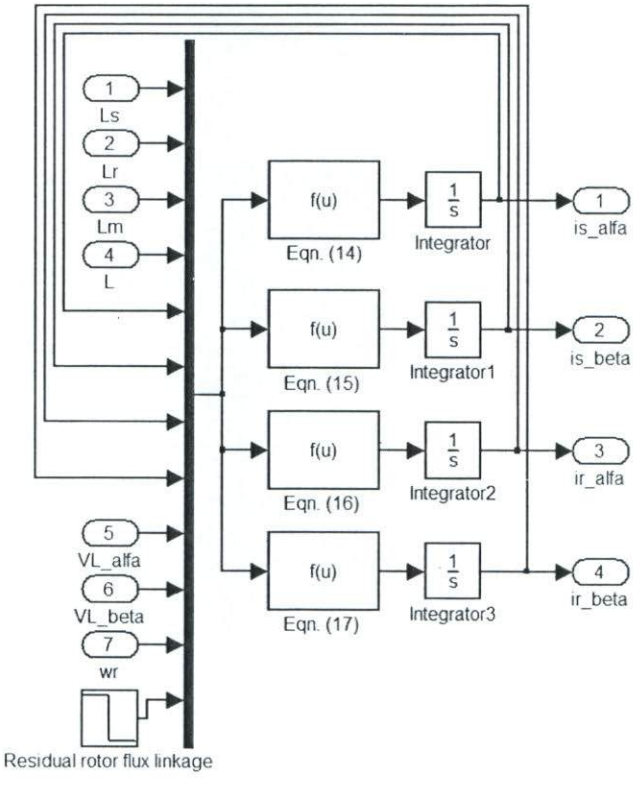

Fig. 4 Sub-system blocks of stator and rotor currents.

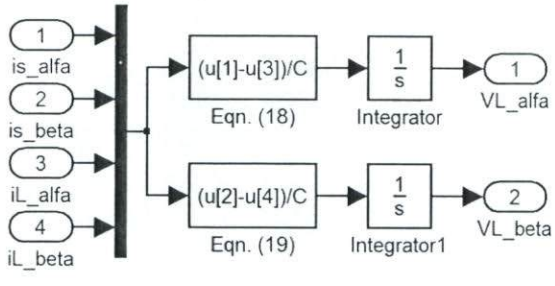

Fig. 5 Sub-system blocks of load voltages.

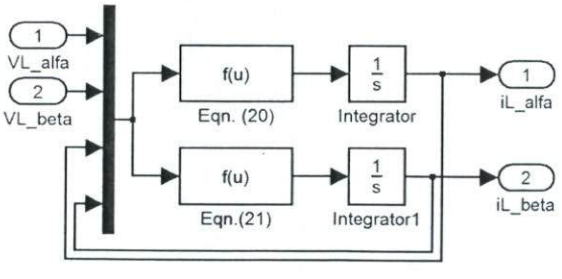

Fig. 6 Sub-system blocks of load currents.

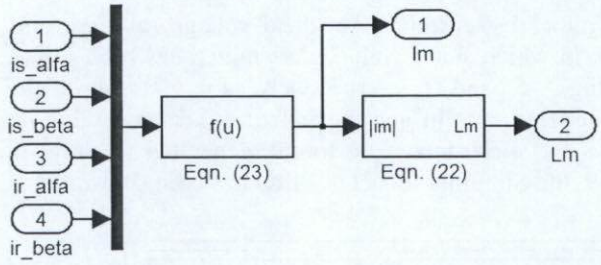

Fig. 7 Sub-system blocks of magnetizing current and magnetizing inductance.

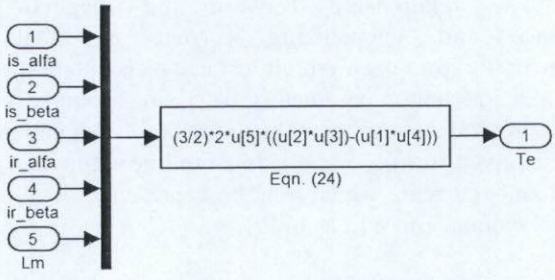

Fig. 8 Sub-system blocks of electromagnetic torque.

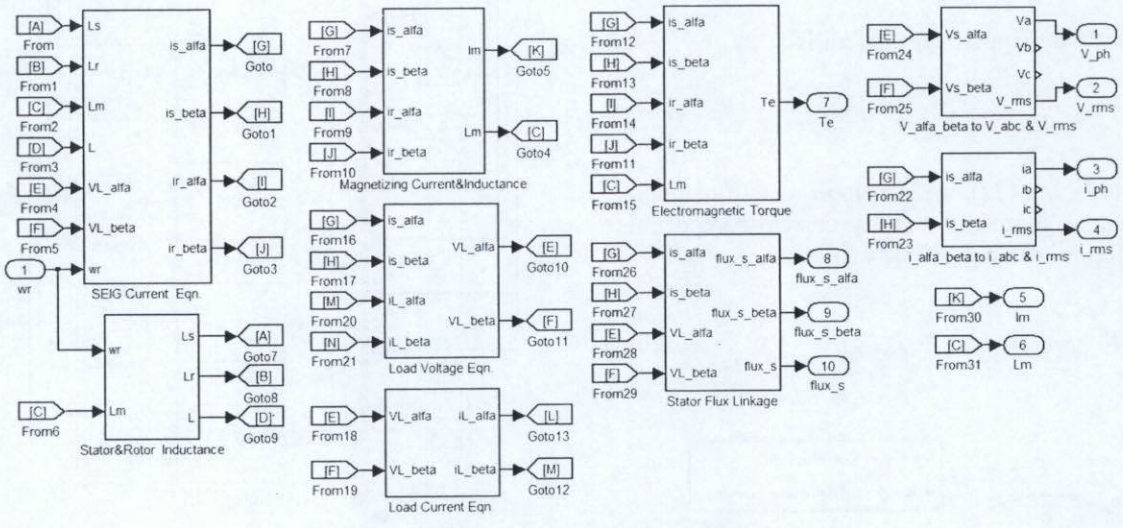

Fig. 9 Simulink model of proposed in this paper.

4. Simulation Results

The simulation in this paper has been developed in Matlab/Simulink environment. In the model is variable prime mover speed from 900 rpm to 1800 rpm and the capacitance is fixed. The induction machine parameters used in the simulation are given in Table 1.

Table 1
Induction machine parameters

3-phase	2.2 kW	$R_s = R_r = 0.9\ \Omega$
60 Hz	4-poles	$L_{ls} = 3.57$ mH
220 V	8 A	$L_{lr} = 3.57$ mH
$N_r = 1760$ rpm.	$C = 90\ \mu$F	$L_m = 141.56$ mH

The simulation result of the start-up characteristic under full-load is shown in Fig. 10. It can be seen that the magnetizing current increases from zero the magnetizing inductance increases, reaches its peak value, then start to decrease and finally reaches its saturated value.

Fig. 11 (a) shows the build-up voltage acceleration and rms voltage are start-up, respectively. Fig. 11 (b) shows the prime mover speed of the proposed method when the speed reference is fixed at 1800 rpm. It can be seen that the speed is well regulated in transients. Fig. 11 (c) shows the phase and rms stator currents under start-up at full-load, respectively. It is seen that the stator current is somewhat unstable close to 0 rpm. As the result, in Fig. 11 (d), it is seen that the electromagnetic torque is generated from 0 Nm to -5 Nm. The torque increases during start-up operation.

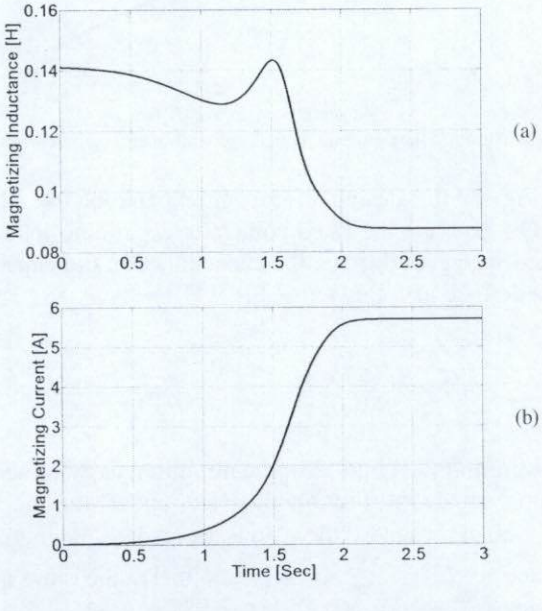

Fig. 10 Simulation results of the start-up SEIG to 1800 rpm. under full-load condition: (a) magnetizing inductance (b) magnetizing current.

As shown in Fig. 12 (a), the build-up of α–β axis stator flux linkages during the self-excitation process. The stator flux linkages continue to grow until they reach steady-state values whish are the saturated stator flux-linkage and its circular trajectory. The value of the stator flux linkage amplitude is 0.5 Wb, as shown in Fig. 12 (b).

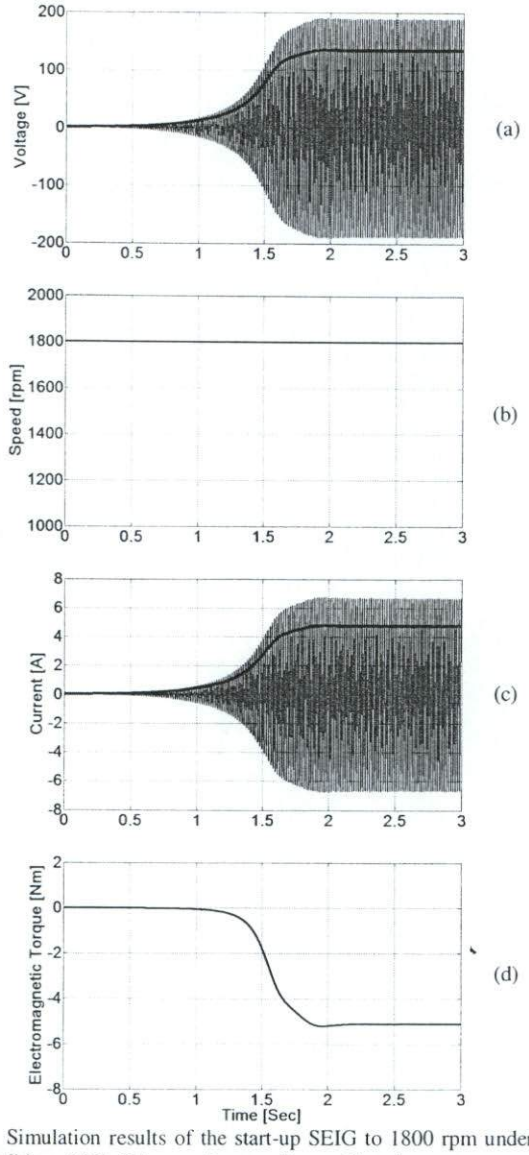

Fig. 11 Simulation results of the start-up SEIG to 1800 rpm under full-load condition: (a) build-up and rms voltages (b) prime mover speed (c) phase and rms stator currents (d) electromagnetic torque.

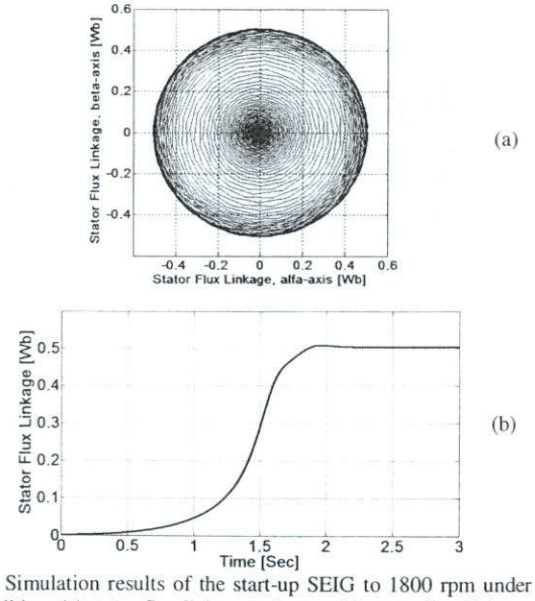

Fig. 12 Simulation results of the start-up SEIG to 1800 rpm under full-load condition: (a) stator flux linkage trajectory (b) stator flux linkage.

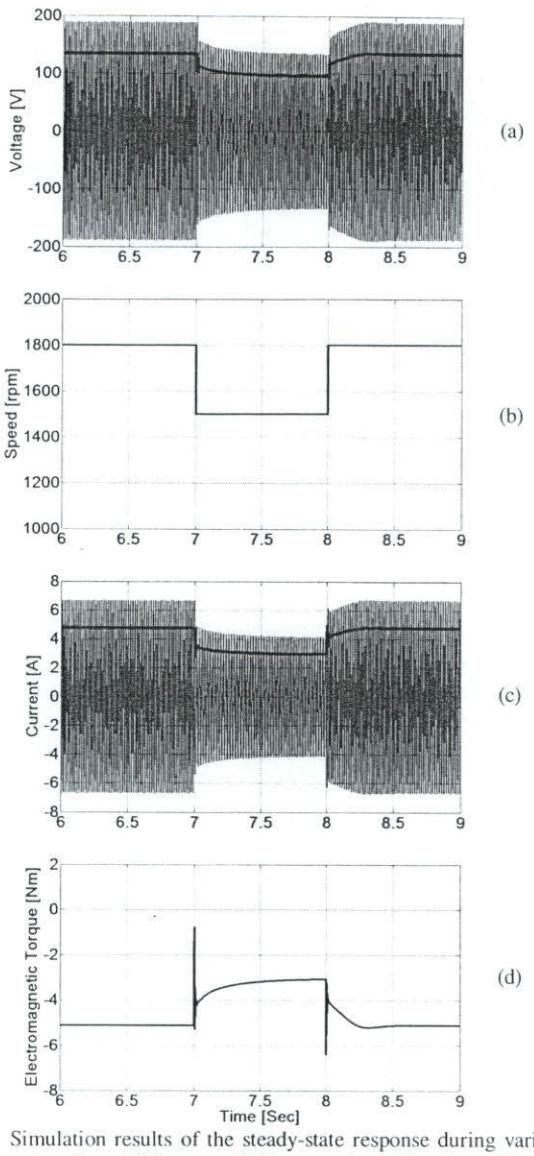

Fig. 13 Simulation results of the steady-state response during variable speed operation from 1800 rpm to 1500 rpm under full-load condition: (a) phase and rms voltages (b) prime mover speed (c) phase and rms stator currents (d) electromagnetic torque.

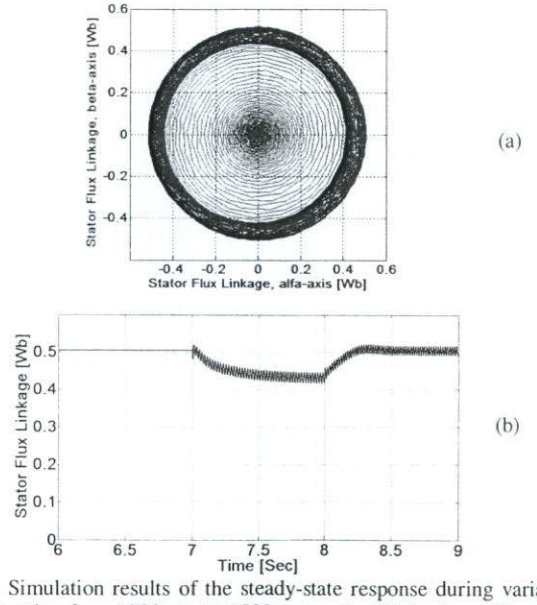

Fig. 14 Simulation results of the steady-state response during variable speed operation from 1800 rpm to 1500 rpm under full-load condition: (a) stator flux linkage trajectory (b) stator flux linkage.

The transient responses are presented in Fig. 13, when the prime mover speed is changed from 1800 rpm to 1500 rpm and then changed from 1500 rpm to 1800 rpm, as shown in Fig 13 (b). Fig 13 (a) shows, the phase and rms voltage, it can be seen that the voltage is unregulated in transient. Figs. 13 (c) and (d) show phase and rms stator current, and electromagnetic torque, respectively. As the result, it is seen that the current amplitude and torque amplitude decreases during transient operation.

As shown in Fig. 14 (a), the stator flux linkage trajectory is plotted in stator α–β plane and its very circular and smooth stator flux linkage is observed in both constant speed and variable speed operation. Fig. 14 (b) shown the stator flux linkage transients step prime mover speed changed from 1800 rpm to 1500 rpm and from 1500 rpm to 1800 rpm. It can be seen that, small change in stator flux linkage amplitude.

5. Conclusions

This paper has presented design and development dynamic modeling of the self-excited induction generator using Matlab/Simulink. The paper has proposed model analyses the steady-state and transient characteristics with the variable speed, and constant load. The simulation results have shown that, variation of magnetizing inductance and magnetizing current, build-up voltage, speed, stator current, electromagnetic toque and stator flux linkage of SEIG under variable and constant speed. The model gives good dynamic and steady-state performance of SEIG. Further work will on the development direct torque control (DTC) to regulate the output stator flux linkage, voltage and frequency of SEIG.

References

[1] R. C. Bansal, "Three-Phase Self-Excited Induction Generator: An Overview", *IEEE Transactions on Energy Conversion*, vol. 20, no. 2, pp. 292-299, June 2005.

[2] T. Ahmed, O. Noro, E. Hiraki, and M. Nakaoka, "Terminal Voltage Regulation Characteristics by Static Var Compensator for a Three-Phase Self-Excited Induction Generator", *IEEE Transactions on Industry Applications*, vol. 40, no. 4, pp. 978-988, July/August 2005.

[3] D. Seyoum, C. Grantham, and M. F. Rahman, "The Dynamic Characteristics of an Isolated Self-Excited Induction Generator Driven by a Wind Turbine", *IEEE Transactions on Industry Applications*, vol. 39, no. 4, pp. 936-944, July/August 2003.

[4] G. V. Jayaramaiah and B. G. Fernandes, "Novel Voltage Controller for Stand-alone Induction Generator using PWM-VSI", *IEEE Conference on Industry Applications*, vol. 1, pp. 204-208, October 2006.

[5] C. Grantham, D. Sutanto, and B. Bismail, "Steady-state and Analysis of Self-Excited Induction Generators", *IEE Proceedings on Electric Power Applications*, vol. 136, no. 2, pp. 61-68, March 1989.

[6] R. J. Harrington and F. M. M. Bassiouny, "New Approach to Determine the Critical Capacitance for Self-Excited Induction Generators", *IEEE Transactions on Energy Applications*, vol. 13, no. 3, pp. 244-249, September 1998.

[7] O. Ojo, "Minimum Airgap Flux Linkage Requirement for Self-Excitation in Stand-alone Induction Generators", *IEEE Transactions on Energy Conversion*, vol. 10, no. 3, pp. 484-492, September 1995.

[8] G. R. Slemon, "Modelling of Induction Machines for Electric Drives", *IEEE Transactions on Industry Applications*, vol. 25, no. 6, pp. 1126-1131, November/December 1989.

[9] T. Ahmed, K.Nishida and M. Nakaoka, "Advance Control for PWM Converter and Variable-Speed Induction Generator", *IET Electric Power Applications*, vol. 1, pp. 239-247, March 2007.

Appendix

List of Symbols

$v_{s\alpha}, v_{s\beta}, v_{r\alpha}, v_{r\beta}$	Stator and rotor voltages in α and β axis
$V_{C\alpha}, V_{C\beta}$	Capacitor voltages in α and β axis
$V_{C\alpha 0}, V_{C\beta 0}$	Initial capacitor voltages in α and β axis
$v_{L\alpha}, v_{L\beta}$	Inductive load voltages in α and β axis
$i_{s\alpha}, i_{s\beta}, i_{r\alpha}, i_{r\beta}$	Stator and rotor currents in α and β axis
$i_{C\alpha}, i_{C\beta}$	Capacitor currents in α and β axis
$i_{L\alpha}, i_{L\beta}$	Inductive load currents in α and β axis
i_m, I_m	Magnetizing current
$\psi_{r\alpha}, \psi_{r\beta}$	Rotor flux linkages in α and β axis
$\psi_{r\alpha 0}, \psi_{r\beta 0}$	Residual rotor flux linkages in α and β axis
$\omega_r\psi_{r\alpha}, \omega_r\psi_{r\beta}$	Rotating voltages in α and β axis
R_s, R_r	Stator and rotor resistances
R_L	Load resistance
L_s, L_r	Stator and rotor inductances
L_{ls}, L_{lr}	Stator and rotor linkages inductance
L_L	Load inductance
L_m	Magnetizing inductance
N_r	Rotor speed
ω_r	Electrical rotor angular speed
T_e	Electromagnetic torque
p_p	Number of pole pairs
p	*d/dt*, the differential operator

Yuttana Kumsuwan received the M.Eng. degree in electrical engineering from King Mongkut's Institute of Technology Ladkrabang (KMITL), Bangkok, Thailand, in 2001. and the Ph.D. degree in electrical engineering from the Chiang Mai University, Chiang Mai, Thailand, in 2007. From October 2007 to March 2008, he was a visiting Scholar with the Texas A&M University. Currently, he is a lecture in the Department of Electrical Engineering, Rajamangala University of Technology Lanna Tak Campus and Chiang Mai University. His research interests are in power electronics, electric drives and power quality.

Watcharin Srirattanawichaikul received the B.Eng. degree (First Class Honors) in electrical engineering from King Mongkut's Institute of Technology Ladkrabang (KMITL), Bangkok, Thailand, in 2006. He is currently studying toward his M.Eng. degree in Electrical Engineering at Chiang Mai University. His research interests are in power electronics, electric drives, control systems and power quality.

Suttichai Premrudeepreechacharn (S'91-M'97) received the B.Eng. degree in electrical engineering from Chiang Mai University, Chiang Mai, Thailand, in 1988 and the M.S. and Ph.D. degree in electric power engineering from Rensselaer Polytechnic Institute, Troy, NY, in 1992 and 1997, respectively. Currently, he is an Associate Professor with the Department of Electrical Engineering, Chiang Mai University. His research interests include power electronics, electric drives, power quality, high-quality utility interfaces and artificial-intelligence-applied power system.